Assessing Root System Architecture of Wheat Seedlings Using A High-Throughput Root Phenotyping System

E. Adeleke[1], R. Millas[1], W. McNeal[1], J Faris[2] and A. Taheri[1]

[1]. Department of Agricultural and Environmental Sciences, Tennessee State University, Nashville, TN 37209

2. USDA-ARS Cereal Crops Research Unit. Edward T. Schafer Agricultural Research Center. 1616 Albrecht BLVD N. Fargo, ND 58102

Abstract

Background and aims

Root system architecture is a vital part of the plant that has been shown to vary between species and within species based on response to genotypic and/or environmental influences. The root traits of wheat seedlings is critical for the establishment and evidently linked to plant height and seed yield. However, plant breeders have not efficiently developed the role of RSA in wheat selection due to the difficulty of studying root traits.

Methods

We set up a root phenotyping platform to characterize RSA in 34 wheat accessions. The phenotyping pipeline consists of the germination paper-based moisture replacement system, image capture units, and root-image processing software. The 34 accessions from two different wheat ploidy levels (hexaploids and tetraploids), were characterized in ten replicates. A total of 19 root traits were quantified from the root architecture generated.

Results

This pipeline allowed for rapid screening of 340 wheat seedlings within 10days. Also, at least one line from each ploidy (6x and 4x) showed significant differences ($P < 0.05$) in measured traits except in mean seminal count. Our result also showed strong correlation (0.8) between total root length, maximum depth and convex hull area.

Conclusions

This phenotyping pipeline has the advantage and capacity to increase screening potential at early stages of plant development leading to characterization of wheat seedling traits that can be further examined using QTL analysis in populations generated from the examined accessions.

Keywords

Root system architecture, high-throughput phenotyping, root traits, *Triticum* sp., germination paper-based system

Introduction

Roots serve as boundaries between plants and complex soil mediums. Aside from anchoring the plant to soil medium (Khan *et al.*, 2016), another major function of the root is to provide plant access to nutrient and water uptake. Roots are also essential for forming symbioses with

beneficial microbes in the rhizosphere and used as storage organs (Smith and De Smet, 2012; Khan *et al.*, 2016). Therefore, roots are critical in the maintenance of plant health. Many environmental factors interact with soils leading to the spatial and temporal heterogenous nature of the soil (Meister *et al.*, 2014). This spatial heterogeneity makes studying the roots in soil a multifaceted challenge. The spatial distribution of roots in soil under field conditions demonstrates a considerable amount of variability since roots respond to heterogeneity of the soil and environmental cues allowing plants to overcome challenges posed by biotic or abiotic factors in soil environment (Smith and De Smet, 2012). This spatial distribution of the root system in soil is referred to as root system architecture (RSA). RSA usually describes the morphological and structural organization of the root (Lynch *et al.*, 1995). RSA is important for plant productivity because it determines the plant's ability to successfully access major heterogenous edaphic resources (de Dorlodot *et al.*, 2007). Therefore, RSA has a direct influence on grain yield.

Wheat is a major cereal crop of global importance and, is grown in temperate zones and has remained a worldwide staple food (Shewry, 2009). It belongs to the *Triticum* genus, which includes species such as *T. aestivum* ssp. *aestivum* L. (common wheat, $2n = 6x = 42$, AABBDD genomes), an allohexaploid and the most cultivated wheat species in the world accounting for 95% of global wheat production (Mayer, 2014); *T. turgidum* ssp. *durum* (Desf.) Husnot (durum wheat, $2n = 4x = 28$, AABB genomes), a tetraploid that is the second most cultivated wheat species accounting for 5-8% of global wheat production (Boyacioglu, 2017); and *T. turgidum* ssp. *dicoccum* (Schrank) Schübl (cultivated emmer wheat, $2n = 4x = 28$, AABB genomes) a tetraploid that is one of the earliest crops domesticated in the Near East (Weiss and Zohary, 2011). So far, most wheat breeding programs have focused on aboveground phenotypic traits while ignoring the belowground traits. Although it is easier for breeders to consider aboveground traits because they are the most visible to the eye, belowground traits should not be ignored because they play equally important roles in plant productivity (Smith and De Smet, 2012; Khan *et al.*, 2016).

In cereal grains, the radicle emerges first and is covered with a protective sheath called the coleorhiza (Shu *et al.*, 2016; Ma *et al.*, 2017). After the roots have extended somewhat further, the coleoptile emerges and grows rapidly. The seedling will then possess a unique RSA (Atkinson *et al.*, 2015) by the time they are at the two-leaf stage (Figure 1), and this has a major impact on the early establishment of the seedling and its productivity at later growth stages.

For wheat to grow and produce enough yield, it is important to understand and select unique traits in RSA as well using aboveground traits. Abiotic stresses due to climate change have affected wheat productivity by limiting the uptake of nutrients and water (de Dorlodot *et al.*, 2007). This is one reason that progress in obtaining wheat varieties with increased yields has been hindered (Fischer and Edmeades, 2010; Richard *et al.*, 2015). One way to alleviate the adverse effects of these factors on wheat yield is to select unique traits and manipulate in the underlying genes associated with wheat RSA so as to optimize the water and nutrient uptake. Although root phenotyping is critical to optimizing RSA in crops, the study of roots in the field is still in its infancy. High-throughput screening can expedite the selection of novel traits for crop

improvement in plant breeding (Richard *et al.*, 2015). However, high throughput screening of root traits is often limited by the lack of suitable phenotyping growth systems (Joshi *et al.*, 2017). Therefore, the main objective of this study was to develop a high-throughput root phenotyping pipeline and evaluate RSA of seedlings from 34 wheat accessions for different root traits.

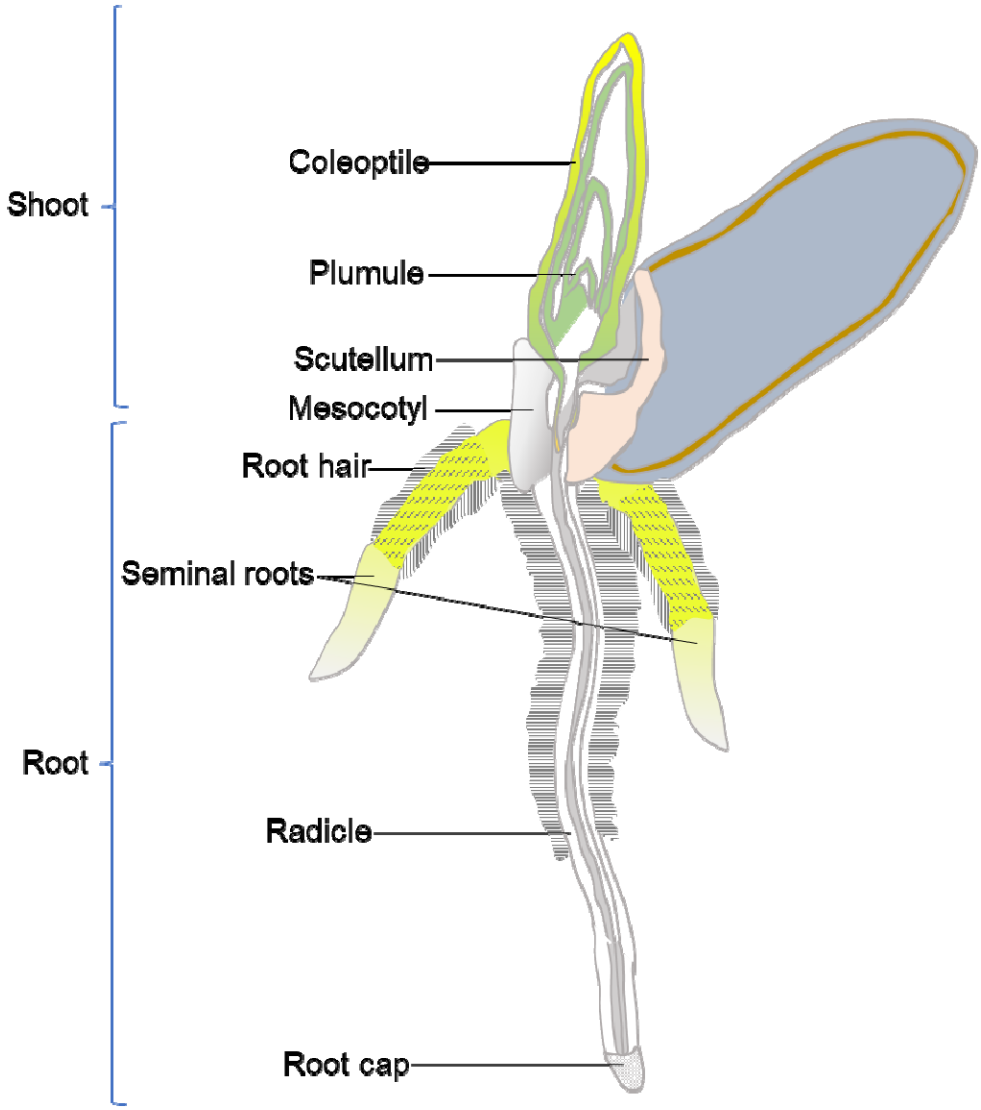

Figure 1. Annotated diagram of germinating 4-day-old wheat grain. The kernel is showing root development that includes root cap, radicle, seminal roots, and root hairs; and shoot development that includes mesocotyl, plumule, and coleoptile at Zadok's growth stage 07 (Zadok et al., 1974).

Methods

Phenotyping of the 34 wheat accessions was divided into three stages, first, setting up the experiment on the platform; second, acquisition of RSA images; and third, analysis of acquired images using open source software (RootNav) (Pound *et al.*, 2013) (Figure 4).

The 34 accessions from different wheat species were obtained from USDA-ARS cereal crop research unit (Fargo, ND, USA) and were divided into two separate groups based on their ploidy level (hexaploid vs tetraploid) (Supplementary Table 1). The hexaploid category was made up of common wheat, spelt wheat and synthetic hexaploid wheat (SHW). In this experiment, SHW lines were selected for root phenotyping with the accession Largo selected as the reference accession based on SHW biomass uniqueness and density (Li *et al.*, 2018). The tetraploid group of accessions consisted of durum (*T. turgidum* ssp. *durum*), Persian (*T. turgidum* ssp. *carthlicum*), cultivated emmer (*T. turgidum* ssp. *dicoccum*) and wild emmer (*T. turgidum* ssp. *dicoccoides*) wheat. For the tetraploid group, the durum line Rusty was selected as the reference accession.

Experimental design and seed treatment

Each accession was planted in ten replicates in a completely randomized design. The seeds were surface sterilized in a chemical hood (Labconco Inc., MO, USA) using the chlorine gas (vapor-phase) method used by Clough and Bent (1998). Ten seeds (or more) were placed in open Petri dishes (previously labeled with chlorine resistant markers) in a 10L desiccator jar. A 3ml aliquot of 12N HCl was added to a 250ml-beaker containing 100 ml of 8.3% sodium hypochlorite before sealing the desiccator. The seeds remained in the desiccator for 4 hours.

Design of experimental platform

A schematic illustration of the stages and flow of the experimental system is presented in Figure 2. We developed a growth pouch system based on the earlier platform designed by Hund et al. (2009) for maize. Each sterilized seed was placed into a germination paper pouch, that was constructed from blue germination paper (21.6 x 28 cm; Anchor Paper Company, St Paul, MN, USA) inserted into Staples® standard clear polypropylene sheet protectors (Staples Inc, MA, USA) (Figure 2, 3A). The bottom edges of these sheet protectors were removed to allow for capillary movement of distilled water and nutrient solution up the germination papers. Two germination pouches were then firmly held to either side of a clear stiff acrylic plate (0.5 x 24 x 30 cm; Acme Plastic Woodland Park, NJ, USA) with a rubber band and a binder clip (Staples Inc, MA, USA) (Figure 3A). The acrylic plates also had extended overhangs (0.5 x 1.5 x 1.0 cm) that fit into a metal support frame that was situated in the top of a customized black polypropylene tank (54.5 x 42.5 x 6.0 cm) (Figure 3C). The 2-D growth systems hung so that they are positioned about 3 cm deep into the liquid media within the tank (Figure 2-B). The liquid solution consisted of 12L of distilled water that was interchanged with modified one-quarter Hoagland's solution (Hoagland and Arnon, 1950) three days after germination. The composition of the nutrient solution was 1.25mM KNO_3; 0.625mM KH_2PO_4; 0.5mM $MgSO_4$; 0.5mM $Ca(NO_3)_2$; 17.5µM H_3BO_3; 5.5 µM $MnCl_2$; 0.5µM $ZnSO_4$; 0.062µM Na_2MoO_4; 2.5µM $NaCl_2$; 0.004µM $CoCl_2$; and 12.5µM Fe-EDTA. The final pH of the nutrient solution was adjusted to pH 6.2.

A single seed from each accession was placed into a germination paper pouch at 2.5 cm below the top with the crease-side down at about a 45^{o} orientation from the vertical plane (Figure 4A). Positioning the seed at this angle provided two main benefits. First, it allowed the phototrophic response of the coleoptile to align with the vertical plane without rerouting its mesocotyl. Second, the position also benefitted the seedling RSA by supporting root emergence away from the germination paper, resulting in easier image acquisition. After 7 days, with almost all seedlings at growth stage 10 (Zadoks *et al*., 1974), each growth pouch was removed from the platform, the polypropylene sheets were cut open on one side, and a side of each sheet was carefully opened to reveal the blue germination paper.

Imaging and analysis

Imaging of the roots was carried out using a Flatbed scanner (HP Inc, USA). The acquired images were saved as standardized compressed image formats (JPG files) which were then imported as new files into the RootNav software. Each image is then converted to a probability map (inverted images) in the software with the root images represented as clustered groups of pixels using the gaussian mixture model based on the varying intensities of the pixels (Pound *et al*., 2013). The RootNav allows expectation maximization clustering to assign the best appearance likelihood of the pixels from root images against the background creating a model that can be fit from the seed point (source) to the root apices.

The RSA images acquired from the wheat seedling were then semi-automatically measured with RootNav software and predefined model setting for wheat seedling was used to acquire measurements of the traits. The root traits that were measured for each replicate included: total length (summation of all the root length – mm), seminal length (the total length of seminal roots – mm), lateral length (the total length of lateral roots – mm), mean seminal length (mean value of the total length of the seminal roots – mm), mean lateral length (mean value of the total length of lateral roots – mm), seminal count (number of seminal roots), lateral count (number of lateral roots), mean seminal count (mean value of the total number of seminal roots), mean lateral count (mean value of the total number of lateral roots), average seminal emergence angle (measurement of emergence angle of the seminal roots – degrees), average lateral emergence angle (measurement of emergence angle of the lateral roots – degrees), average seminal tip angle (mean value of the measurement of angle in the seminal root tips – degrees), average lateral tip angle (mean value of the measurement of angle in the lateral root tips – degrees), root tip angle (the measurement of angle in the seminal root tips – degrees), maximum width (the furthermost width of the root system along horizontal axis – mm), maximum depth (the furthermost depth of the root system along vertical axis – mm), width-depth ratio (the ratio of the maximum width to the maximum depth of the root system), centroid (the coordinates of the center of mass of root system along the horizontal and vertical axes – mm), convex hull area (the area of the smallest convex polygon covering the boundaries of the root system – mm^2), and tortuosity (the average curvature of the seminal roots).

166 Supplementary Table 1. The common name, taxonomy, origin, and source of 34 different accessions assessed for its seedlings RSA.

Accession	PI/CItr	Common name	Taxon	Subspecies	Ploidy	Origin
Largo	CItr 17895	Synthetic hexaploid wheat	*Triticum turgidum* x *Aegiliops tauschii*	Synthetic	6x	U.S., North Dakota
ND495	N/A	Common wheat	*Triticum aestivum*	*aestivum*	6x	U.S., North Dakota
Grandin	PI 531005	Common wheat	*Triticum aestivum*	*aestivum*	6x	U.S., North Dakota
BR34	N/A	Common wheat	*Triticum aestivum*	*aestivum*	6x	Brazil
Chinese Spring	CItr 14108	Common wheat	*Triticum aestivum*	*aestivum*	6x	China
Arina	N/A	Common wheat	*Triticum aestivum*	*aestivum*	6x	Switzerland
Forno	N/A	Common wheat	*Triticum aestivum*	*aestivum*	6x	Switzerland
Sumai 3	PI 481542	Common wheat	*Triticum aestivum*	*aestivum*	6x	China
Chinese Spring-DIC 5B	N/A	Common wheat	*Triticum aestivum*	*aestivum*	6x	U.S., Missouri
Bobwhite	PI 520554	Common wheat	*Triticum aestivum*	*aestivum*	6x	Mexico, CIMMYT
Salamouni	PI 182673	Common wheat	*Triticum aestivum*	*aestivum*	6x	Lebanon
Katepwa	N/A	Common wheat	*Triticum aestivum*	*aestivum*	6x	Canada
M3	N/A	Synthetic hexaploid wheat	*Triticum turgidum* x *Aegiliops tauschii*	Synthetic	6x	Mexico, CIMMYT
M6	N/A	Synthetic hexaploid wheat	*Triticum turgidum* x	Synthetic	6x	Mexico, CIMMYT

			Aegiliops tauschii			
Kulm	PI 590576	Common wheat	*Triticum aestivum*	*aestivum*	6x	U.S., North Dakota
Opata85	PI 591776	Common wheat	*Triticum aestivum*	*aestivum*	6x	Mexico, CIMMYT
TA4152-60	N/A	Synthetic hexaploid wheat	*Triticum turgidum* x	Synthetic	6x	Mexico, CIMMYT
			Aegiliops tauschii			
TA4152-19	N/A	Synthetic hexaploid wheat	*Triticum turgidum* x	Synthetic	6x	Mexico, CIMMYT
			Aegiliops tauschii			
Divide	N/A	Durum wheat	*Triticum turgidum*	*durum*	4x	U.S., North Dakota
Rusty	PI 639869	Durum wheat	*Triticum turgidum*	*durum*	4x	U.S., North Dakota
Ben	N/A	Durum wheat	*Triticum turgidum*	*durum*	4x	U.S., North Dakota
Lebsock	N/A	Durum wheat	*Triticum turgidum*	*durum*	4x	U.S., North Dakota
Langdon	N/A	Durum wheat	*Triticum turgidum*	*durum*	4x	U.S., North Dakota
Altar84	N/A	Durum wheat	*Triticum turgidum*	*durum*	4x	Mexico, CIMMYT
P503	N/A	Spelt wheat	*Triticum aestivum*	*spelta*	6x	Iran
PI193	PI 193833	Cultivated emmer	*Triticum turgidum*	*dicoccum*	4x	Ethiopia
PI410	PI 41025	Cultivated emmer	*Triticum turgidum*	*dicoccum*	4x	Russia
PI947	PI 94749	Persian wheat	*Triticum turgidum*	*carthlicum*	4x	Georgia
PI481	PI 481521	Wild emmer	*Triticum turgidum*	*dicoccoides*	4x	Israel

PI478	PI 478742	Wild emmer	*Triticum turgidum*	*dicoccoides*	4x	Israel
TA106	N/A	Wild emmer	*Triticum turgidum*	*dicoccoides*	4x	Israel
Israel A	N/A	Wild emmer	*Triticum turgidum*	*dicoccoides*	4x	Israel
PI277	PI 277012	Spelt wheat	*Triticum aestivum*	*spelta*	6x	Spain
PI272	PI 272527	Cultivated emmer	*Triticum turgidum*	*dicoccum*	4x	Hungary

167

168

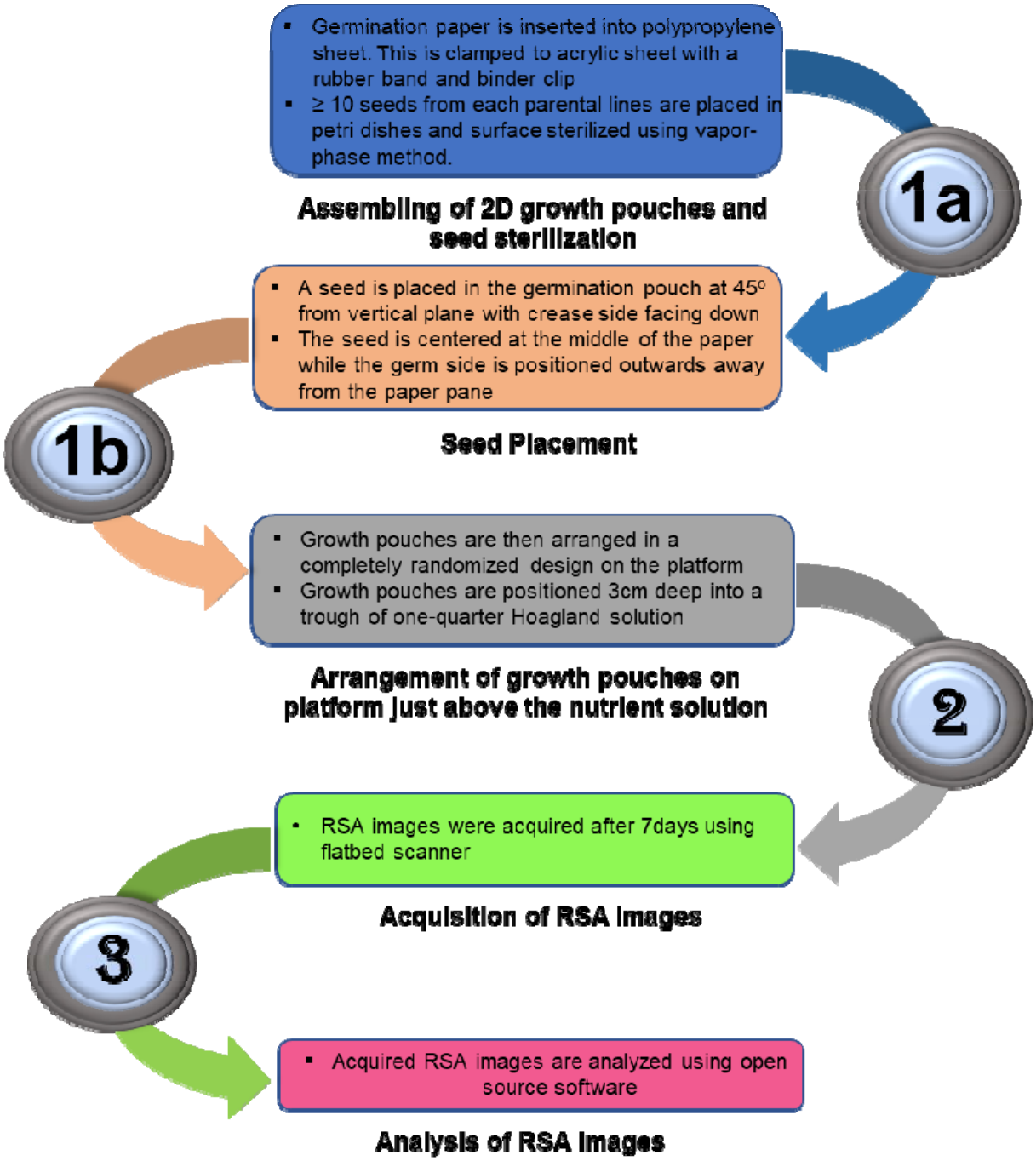

Figure 2. Schematic illustrating the three major steps of the root phenotyping pipeline. The first step is seed sterilization and the assembling of 2D growth pouches (1a), and the placement of seeds in respective pouches accordingly and placement into the tanks (1b). The second step involves the acquisition of RSA images using a flatbed scanner (2). The third step is the analyses of RSA images acquired in the second step (3).

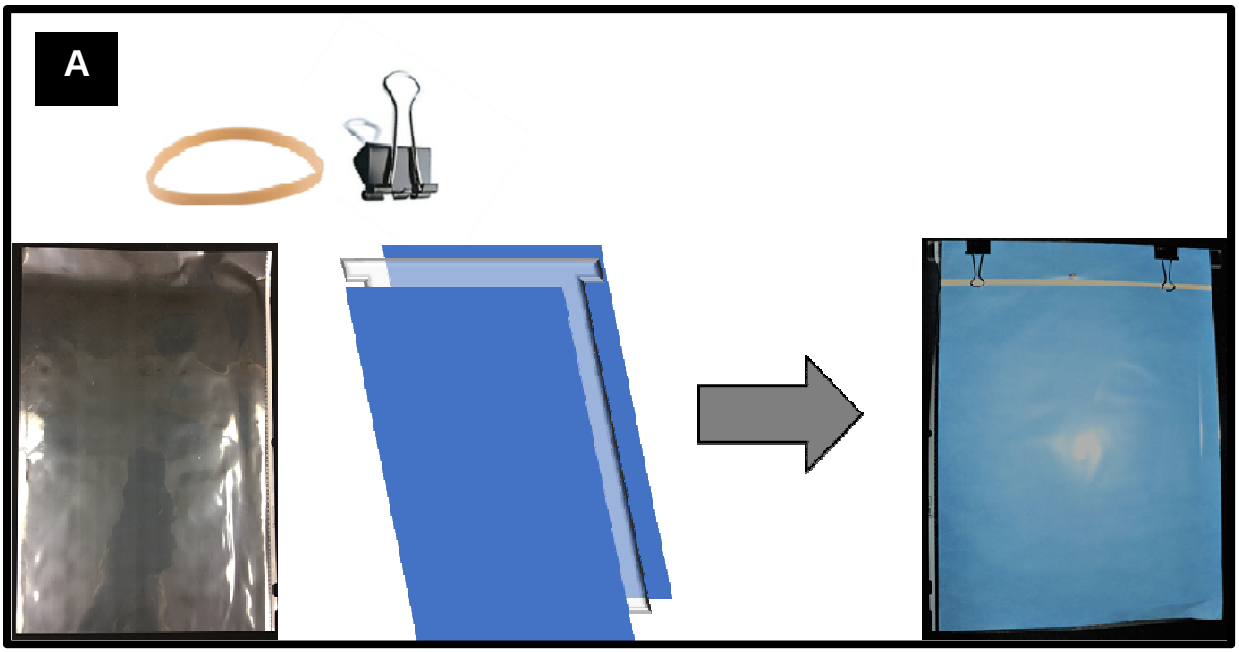

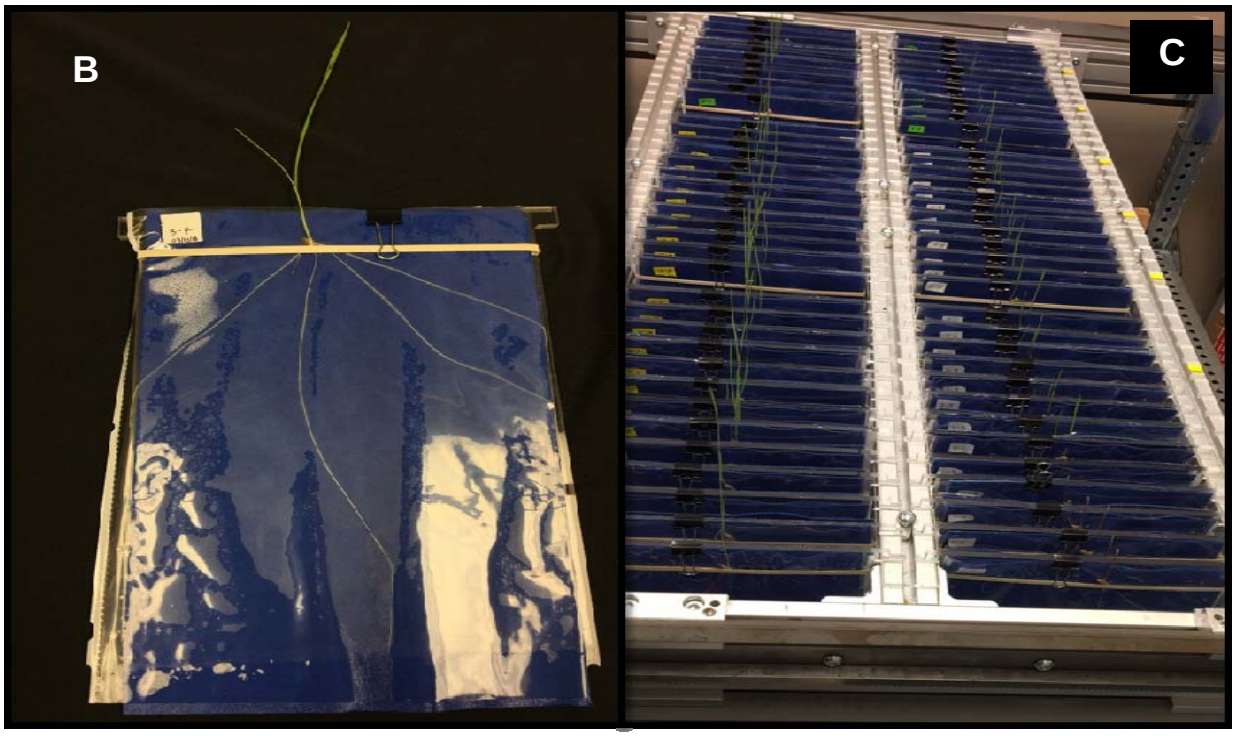

Figure 3. A customized high-throughput seedling root phenotyping platform is showing the growth assembly. The 2-D growth system showing the growth pouch on one side. (A). The growth paper was inserted within the cover sheet that has had the bottom end removed. A rubber band and binder hold two germination pouches firmly in place to the acrylic plate. (B). The germinated seed shows the RSA of the wheat seedling at the two-leaf stage. (C). An assembled 2-D growth system showing growth pouches hanging from a metal frame.

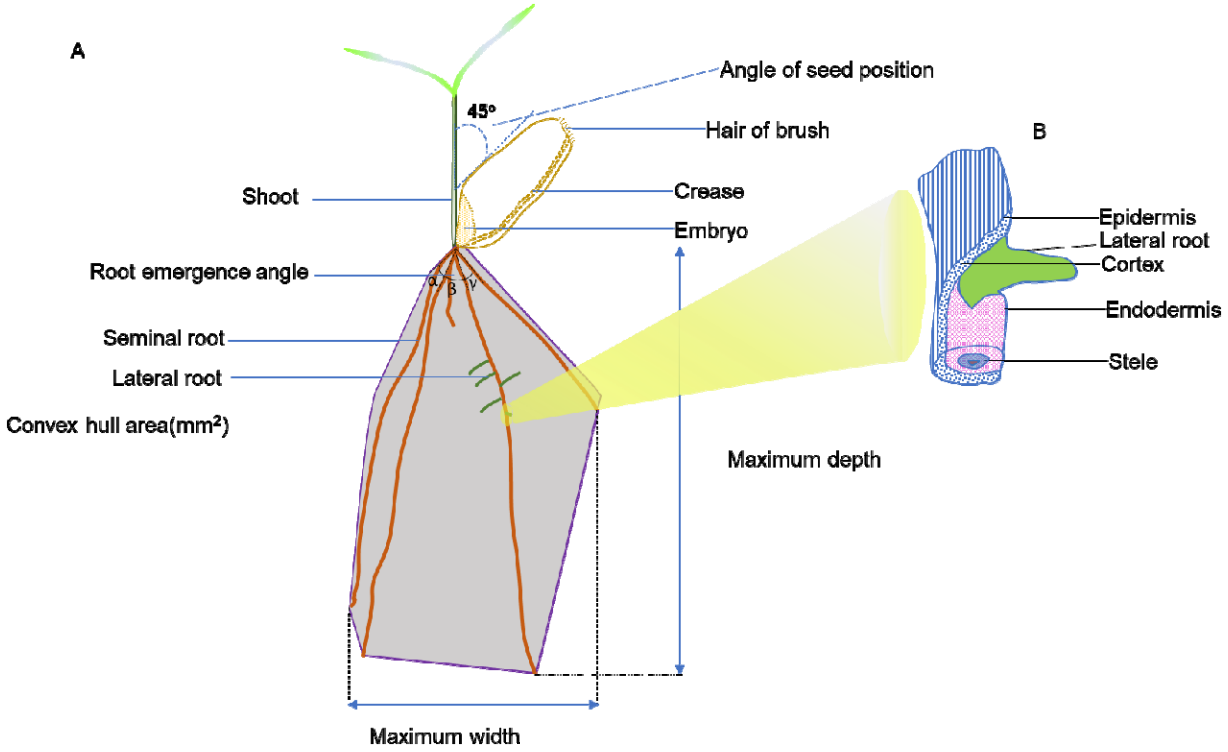

Figure 4. (A) Summary of seedling features within the growth system and positioning of the seed. The positioning of the seed at 45^{o} to the vertical plane of the growth system permitted a precise upward development of the coleoptile and concomitant downward growth of the roots. The crease of the seed is inverted to face the horizontal plane of the pouch thus allowing the roots to grow away from the germination paper (B) Illustration of lateral root emerging from the overlying tissues of the primary seminal root.

Statistical analysis of the results obtained from RootNav was processed and analyzed using IBM SPSS Statistics for Windows, v25.0 (IBM Corp., NY, USA). The results obtained were expressed as mean values for each parental line for each trait. Analysis of variance (ANOVA) was applied to compare the means. Based on the outcome of the ANOVA on all data, Tukey HSD post hoc analysis was performed to separate the means.

Spearman rank correlation coefficients (ρ) was used to determine associations between measured traits. Data analysis and visualization of the mixed model was performed using R software Version 3.4.3.

Results

The root of the wheat seedlings grew freely along the airspace between the clear propylene sheet and the moistened blue absorbent growth paper without growing into the paper. This allowed for capturing of clearly distinguishable root image from the blue germination paper. RootNav

software was used to extract the quantification of RSA traits from the total root images of 312 seedlings that were captured 7 days after planting.

Frequency distribution of germination potential and measured root traits

The germination potential of each PL accessions is shown in Figure 5. The average germination rate of hexaploid was 9.4% higher than the tetraploid wheat accessions. The frequency distribution of the germination potential showed that 85.3% of all accessions exceeded a 90% germination rate (Supplementary Figure S1).

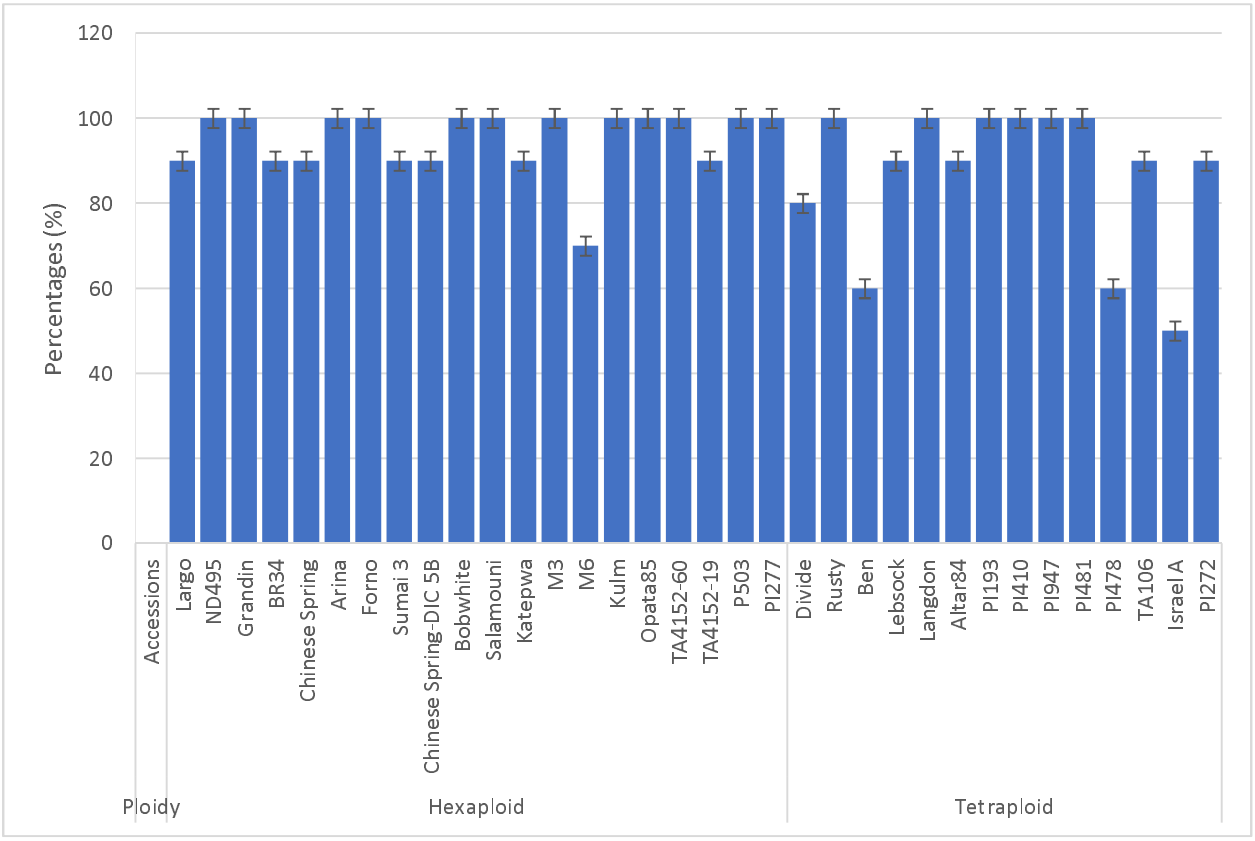

Figure 5. Germination potential for each accession

The frequency histograms of the measured root traits for the 34 accessions are shown in Supplementary Figure S2. There was a strong correlation (0.8) between observed traits of total seminal root length and convex hull area. The average seminal length was strongly correlated (0.8) with maximum depth and centroid while maximum width highly correlated (0.9) with width-depth ratio and convex hull area. The maximum depth also showed a high correlation (0.9) with a centroid (Supplementary Figure S3).

The hexaploid wheat accessions

The non-destructive measurements of the RSA roots showed that the mean total length (Figure 8A) of Salamouni, Katepwa, Kulm, Opata85, TA60, Grandin, P503, Arina, Forno, Sumai3, and Chinese Spring-DIC 5B were significantly longer compared with Largo, which was used as the reference, by 0.9, 1.3, 1.9, 2.1, 1.5, 1.6, 0.9, 1.3, and 1.4 times respectively. The average seminal length (Figure 9A) of Kulm, Opata85, TA60, Grandin, P503, Arina, and Forno compared to Largo were significantly longer by 1.0, 1.0, 1.2, 0.8 1.0, 1.0, and 1.2 times respectively. The mean count of the seminal root (Figure 10A) of Katepwa, Kulm, Opata85, and Grandin was significantly higher compared with Largo by 0.5, 0.4, 0.5 and 0.4 times respectively. The mean maximum width (Figure 11A) showed that Kulm, Opata85, and Grandin were significantly larger compared with Largo by 2.2, 1.4 and 1.7 times respectively. The maximum depth (Figure 12A) of Kulm, Opata85, TA60, Grandin, P503, Arina, Forno, Sumai3, and Chinese Spring-DIC 5B were significantly greater compared with Largo by 0.7, 0.8, 0.8, 0.6, 0.7, 0.7, 1.0, 0.8, and 0.8 times respectively. The width to depth ratio (Figure 13A) of Kulm was significantly larger compared with Largo by 0.9 times. The mean convex hull area (Figure 14 A) of Kulm, Opata85, TA60, Grandin, and Arina were significantly larger compared to Largo by 5.3, 4.8, 3.3, 4.1 and 3.1 times respectively. The vertical coordinate of the centroid (Figure 17A) showed that Kulm, Opata85, TA60, TA19, P503, Arina, Forno, Sumai3, and Chinese Spring-DIC 5B were significantly greater compared with Largo by 0.8, 1.0, 1.2, 0.8, 1.0, 1.1, 1.5, 1.0, 0.9 times respectively.

The tetraploid wheat accessions

Accessions Langdon, PI 193883, PI 41025, PI 94749, and PI 272 were significantly higher in mean total length compared with Rusty (which was used as reference) by 1.4, 1.6, 1.6, 1.8, and 1.4 times respectively (Figure 8B). For mean seminal length, Lebsock, PI 193883, PI 41025, and PI 94749 showed a significantly longer seminal root with 1.5, 1.4, 1.6, and 1.5 times more than Rusty (Figure 9B).

For the mean maximum width, PI 277 showed a significant difference increasing 1.7 times more than Rusty (Figure 11B). For mean maximum depth, PI 193, PI 410 and PI272 showed a significant difference increasing 0.9, 0.8, and 0.8 times more than Rusty respectively (Figure 12B). For the mean width to depth ratio (Figure 13A), the PI 277 showed a significant increase of 1.1 times more than Rusty (Figure 13B).

In other measured root trait, mean convex hull area of PI 193883 significantly increased 3.1 times when compared to Rusty (Figure 14B). Also, for centroid_Y, Lebsock, PI 193, PI 410 and Israel showed a significant difference increasing 1.4, 1.6, 1.5 and 1.6 times respectively.

Discussion

The root phenotyping pipeline examined in this study using a germination paper-based moisture replacement system allowed measurement of important root architectural traits to be collected in an efficient, low-cost, and high-throughput fashion.

The benefit of the root system size

The root system size is the representation of the total root length, seminal count, and the convex hull area. In previous studies, these traits have been positively associated with each other as well as with grain yield of wheat in the field (Liu *et al.*, (2013) and Xie *et al.*, (2017)). We also found a significant correlation between the total root length, maximum depth and the convex hull area in this study. In addition, the average seminal root length showed a significant correlation with both total root length and the convex hull area which agrees with previous findings (Cao *et al.*, 2014) that suggested that deeper penetration of the soil by seedling roots results in better access to soil nutrients and early plant establishment. The total root length and the average seminal root length had strong associations with the Centroid_Y (vertical axis), which is suggested to be responsible for the aboveground vigor and root depth of the plant (Atkinson *et al.*, 2015).

Kulm and Opata85 may be useful for RSA improvement in hexaploid wheat

Kulm is a hard-red spring wheat (HRSW) developed at North Dakota State University, Fargo, ND. Kulm performed the best in our study among all the accessions we examined. Kulm had a higher mean total length, mean average primary length, seminal count and convex hull area making it a suitable candidate for breeding a larger root system and greater spatial distribution. Kulm has been used in previous studies as a parental line for inbred line developments (Mergoum *et al.*, 2009; Ghaffary *et al.*, 2012) with a report affirming its higher yield. Although, Kulm has been found susceptible to some wheat pathogens like septoria tritici blotch (STB) (Ghaffary *et al.*, 2012), *septoria nodorum* blotch (SNB) and tan spot (Faris *et al.*, 2010), it remains a good candidate for selection of grain-end-use quality (Mergoum *et al.*, 2009).

Opata 85 is a commercial spring wheat cultivar developed at International Maize and Wheat Improvement Center (CIMMYT), Mexico (Borner *et al.*, 2002). In our study, the next best accession after Kulm was Opata85 as it produced more roots and an overall architecture that allowed it to occupy more root area. These traits make Opata 85 a suitable breeding candidate for larger root development and improvement of abiotic stress resistance. Opata 85 has been used as a parental line for recombinant inbred lines (RILs) used to map yield traits (Kumar *et al.*, 2007), important agronomic traits (Borner *et al.*, 2002), growth characters (Kulwal *et al.*, 2003), water-logging tolerance in seed germination and seedling growth (YU *et al.*, 2014), and growth duration components (Yu *et al.*, 2015).

The significance of a rapid screening pipeline for measuring seedling root traits

The high throughput root phenotyping pipeline that was developed in this study revealed variation in seedling root traits of both hexaploid and tetraploid wheat accessions. The pipeline allowed us to examine the root system architecture of 340 wheat seedlings using only one out of four sections of our metal scaffoldings that were fitted with three solution tanks. Each section has the capacity to fit-in 84 growth systems that led to screening approximately 168 seedlings for each assembly. The total capacity of the platform can allow phenotypic evaluation of 672 plants per run in the fixed temperature growth room within 10days and this includes the assembling of 2-D growth system and image analysis. Acquisition of root images of 168 seedlings takes approximately 3.5 hours while the semi-automated image analysis using open source software

takes 1.5mins per image. This is similar to findings of Atkinson *et al.*, (2015) who reported ~2mins per image and ~5mins per plant.

The cost of the 2D-growth system is ~ $0.43 per plant with a reusable acrylic sheet of ~ $3.30. The overall growth system assembly for the first time will cost $4.20 with a recurring cost of $0.90 per system. This is 81% lower than the average available market price of seed germination pouches.

Although different phenotyping systems based on germination paper have been reported in previous studies (Hund *et al.*, 2009a; Ingram *et al.*, 2012; Richard *et al.*, 2015), the pipeline described in this study is similar to the pouch and wick hydroponic-based system (Atkinson *et al.*, 2015). However, the pipeline in our study was enhanced by adding vapor sterilization of the seeds; positioning of the wheat seeds at a strategic angle that improved root images; growing two (2) plants per growth system; and utilization of separable solution tanks that can hold up to 4L of nutrient solution and 28 growth systems. The advantage of this type of solution tank is that root response to abiotic stress and different nutrient regimes can be assessed by varying solution constituent.

Future Work

SHW lines have become valuable resources for the genetic improvement of common wheat cultivars (Li *et al.*, 2018). The findings of variation analysis from this study will allow us to investigate segregating mapping populations that will include RILs of M3 and Kulm; and M6 and Opata85. M3 was developed at CIMMYT, Mexico whereas Kulm was developed at North Dakota State University, Fargo, ND. These hexaploids are both spring type with M3 been a synthetic hexaploid while Kulm is a hard-red spring wheat (Ghaffary *et al.*, 2012). The associative mapping population that resulted from the crossing of these two lines (Kulm x M3) resulted in the 105 RILs that will be used in further studies of the hexaploid. Additionally, 114RILs resulting from the hexaploid mapping population of Opata85 x M6 and chromosome substitution lines involving PI 478742, a tetraploid (where individual pairs of chromosomes of wild emmer have been substituted for homologous pairs of chromosomes in background of Langdon durum) will be evaluated to identify the chromosome locations of loci responsible for the differences in RSA traits. Thereafter, molecular markers suitable for marker-assisted selection of these traits will be developed.

Conclusion

In this study, we have studied RSA on 34 different wheat accessions at an early stage of plant development and were able to demonstrate its use in identifying accessions which perform better than others in some of the RSA characters. This study clearly possesses an advantage over the previously reported study because of the advantage and capacity to increase screening potential at early stages of plant development. Also, this pipeline is very simple and provides an opportunity for automation and screening platforms. Availability of mapping populations and high-resolution mapping data from these accessions provides an opportunity for utilizing this pipeline in identifying QTLs linked to RSA in populations segregating in RSA traits.

8

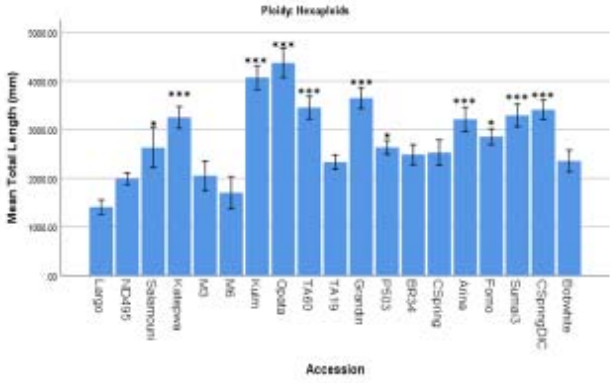

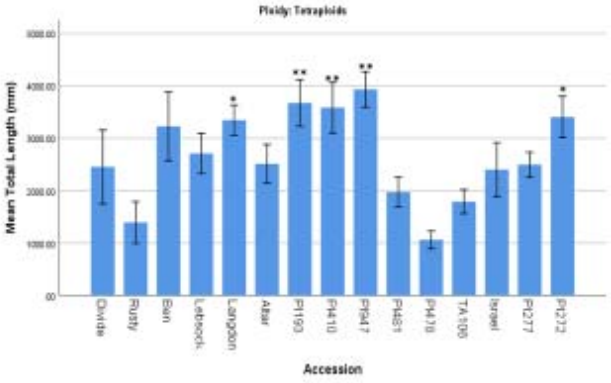

9

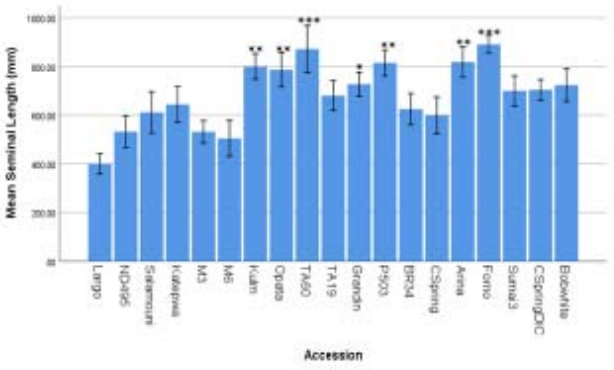

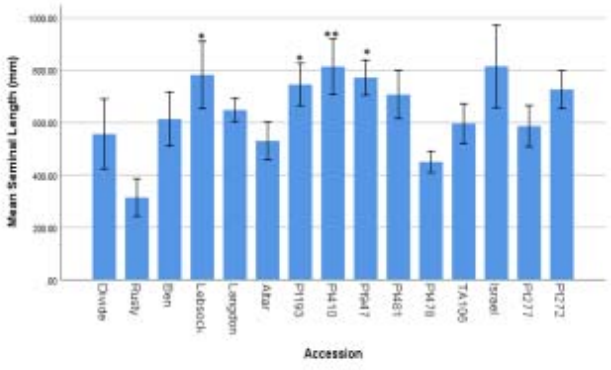

10

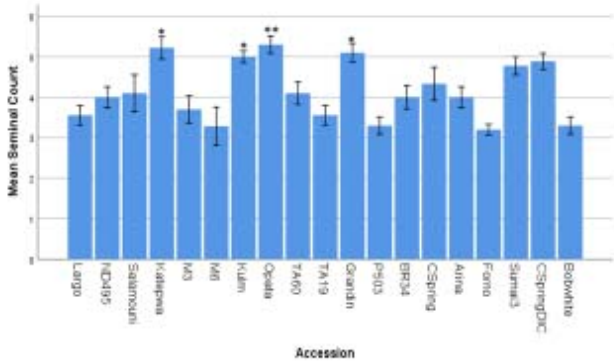

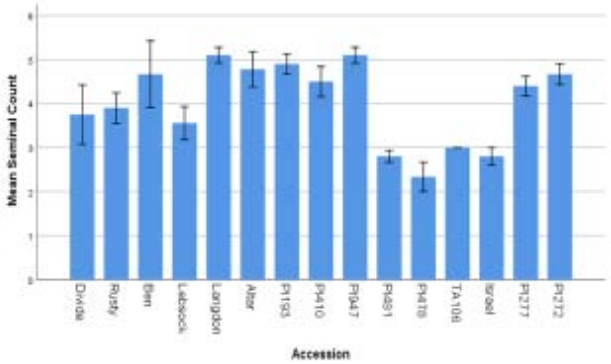

11

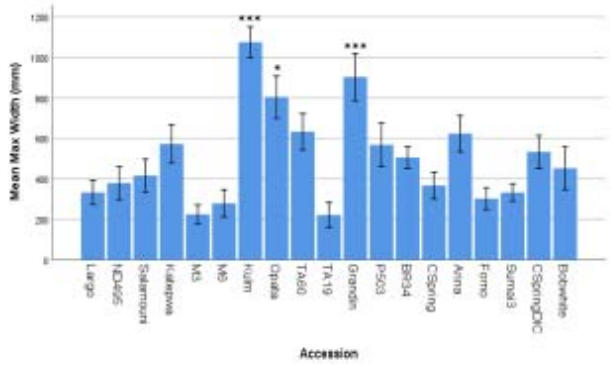

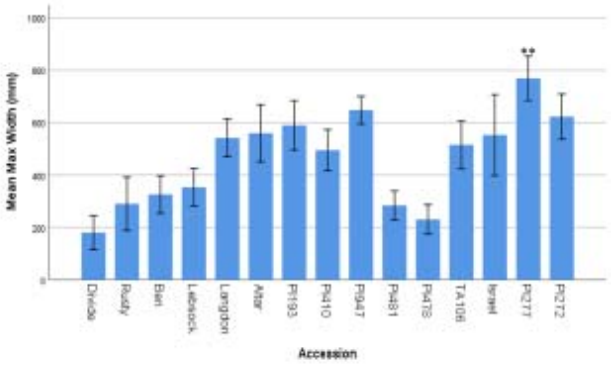

342

343

A

B

12

13

14

15

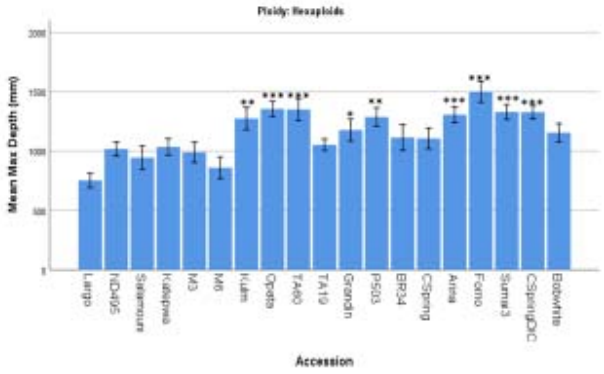

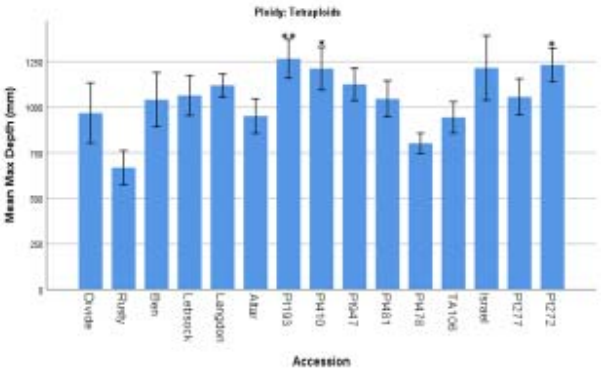

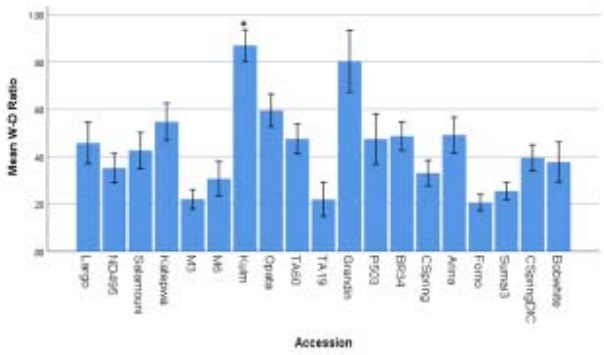

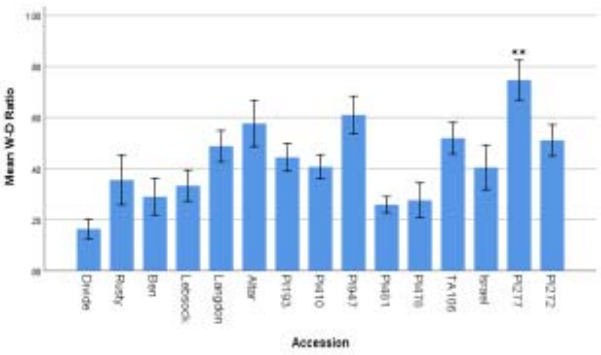

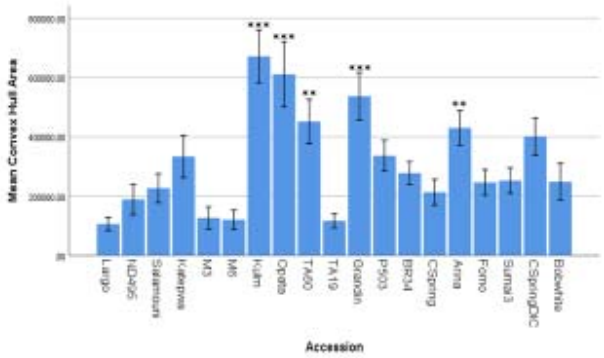

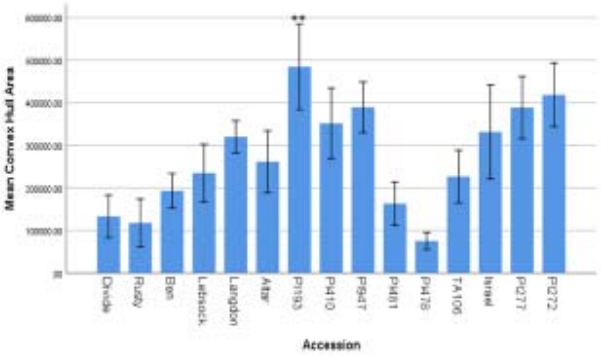

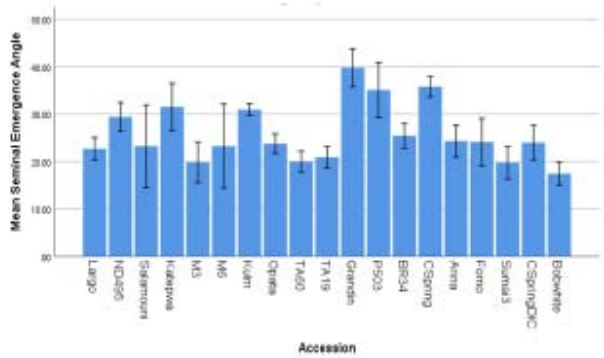

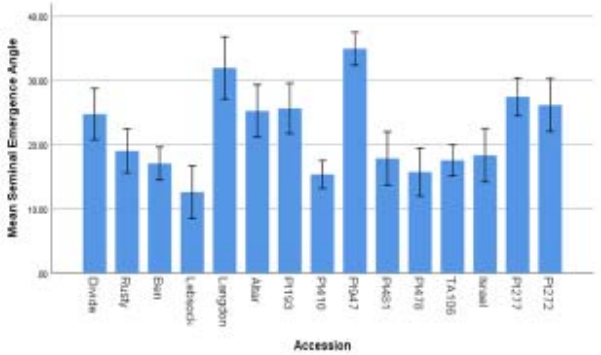

344

345

A

B

16

17

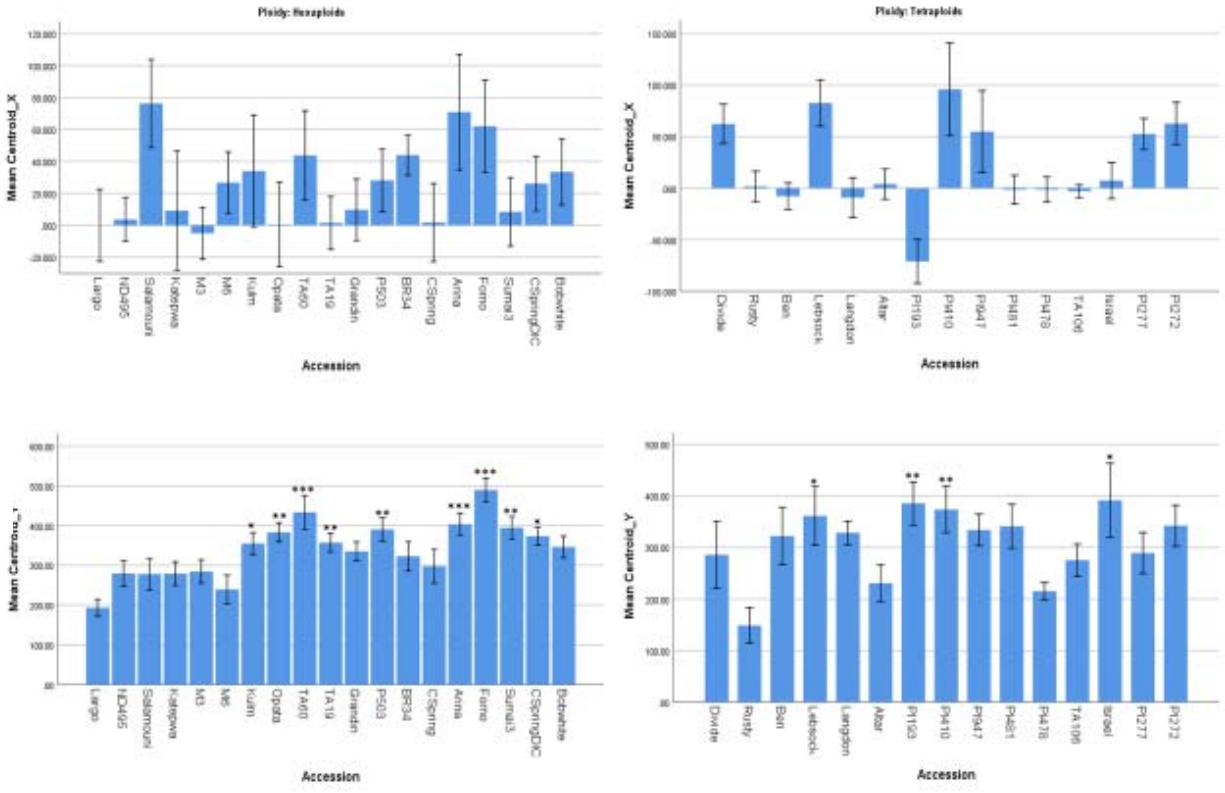

A B

346

347 Figures 8-17. Root system architecture traits measured in 34 parental what accessions.

348

349 References

350 Atkinson, J. A. *et al.* (2015) 'Phenotyping pipeline reveals major seedling root growth QTL in
351 hexaploid wheat', *Journal of Experimental Botany*. Oxford University Press, 66(8), pp. 2283–
352 2292. doi: 10.1093/jxb/erv006.

353 Borner, A. *et al.* (2002) 'Mapping of quantitative trait loci determining agronomic important
354 characters in hexaploid wheat (Triticum aestivum L.)', *TAG Theoretical and Applied Genetics*.
355 Springer-Verlag, 105(6–7), pp. 921–936. doi: 10.1007/s00122-002-0994-1.

356 Boyacioglu, H. (2017) *Global durum wheat use trending upward | World Grain*, *World Grain*
357 *News*. Available at: http://www.world-
358 grain.com/articles/news_home/World_Grain_News/2017/10/Global_durum_wheat_use_trendin.
359 aspx?ID=%7B04F7D478-8010-49E7-A30E-60F63024D10D%7D&cck=1 (Accessed: 13 March
360 2018).

361 Cao, P. *et al.* (2014) 'Further genetic analysis of a major quantitative trait locus controlling root
362 length and related traits in common wheat', *Molecular Breeding*, 33(4), pp. 975–985. doi:
363 10.1007/s11032-013-0013-z.

364 Clough, S. J. and Bent, A. F. (1998) 'Floral dip: a simplified method forAgrobacterium-mediated
365 transformation ofArabidopsis thaliana', *The Plant Journal*. Wiley/Blackwell (10.1111), 16(6),
366 pp. 735–743. doi: 10.1046/j.1365-313x.1998.00343.x.

367 de Dorlodot, S. *et al.* (2007) 'Root system architecture: opportunities and constraints for genetic
368 improvement of crops', *Trends in Plant Science*, 12(10), pp. 474–481. doi:
369 10.1016/j.tplants.2007.08.012.

370 Faris, J. D. *et al.* (2010) 'A unique wheat disease resistance-like gene governs effector-triggered
371 susceptibility to necrotrophic pathogens', *Proceedings of the National Academy of Sciences*,
372 107(30), pp. 13544–13549. doi: 10.1073/pnas.1004090107.

373 Fischer, R. A. (Tony) and Edmeades, G. O. (2010) 'Breeding and Cereal Yield Progress', *Crop
374 Science*. Crop Science Society of America, 50(Supplement_1), p. S-85. doi:
375 10.2135/cropsci2009.10.0564.

376 Ghaffary, S. M. T. *et al.* (2012) 'New broad-spectrum resistance to septoria tritici blotch derived
377 from synthetic hexaploid wheat', *Theoretical and Applied Genetics*, 124(1), pp. 125–142. doi:
378 10.1007/s00122-011-1692-7.

379 Hoagland, D. R. and Arnon, D. I. (1950) *The water-culture method for growing plants without
380 soil; revised D.I. Arnon*. Circular 3. Berkeley: Berkeley, Ca□: The College of Agriculture,
381 University of California, Berkeley. Available at:
382 https://trove.nla.gov.au/work/35388503?q&versionId=44010336 (Accessed: 18 March 2018).

383 Hund, A., Trachsel, S. and Stamp, P. (2009) 'Growth of axile and lateral roots of maize: I
384 development of a phenotying platform', *Plant and Soil*. Springer Netherlands, 325(1–2), pp.
385 335–349. doi: 10.1007/s11104-009-9984-2.

386 Ingram, P. A. *et al.* (2012) 'High-throughput imaging and analysis of root system architecture in
387 Brachypodium distachyon under differential nutrient availability.', *Philosophical transactions of
388 the Royal Society of London. Series B, Biological sciences*. The Royal Society, 367(1595), pp.
389 1559–69. doi: 10.1098/rstb.2011.0241.

390 Joshi, D. C. *et al.* (2017) 'Development of a phenotyping platform for high throughput screening
391 of nodal root angle in sorghum', *Plant Methods*. BioMed Central, 13(1), p. 56. doi:
392 10.1186/s13007-017-0206-2.

393 Khan, M. A., Gemenet, D. C. and Villordon, A. (2016) 'Root System Architecture and Abiotic
394 Stress Tolerance: Current Knowledge in Root and Tuber Crops.', *Frontiers in plant science*.
395 Frontiers Media SA, 7, p. 1584. doi: 10.3389/fpls.2016.01584.

396 Kulwal, P. . *et al.* (2003) 'QTL mapping for growth and leaf characters in bread wheat', *Plant
397 Science*. Elsevier, 164(2), pp. 267–277. doi: 10.1016/S0168-9452(02)00409-0.

398 Kumar, N. *et al.* (2007) 'QTL mapping for yield and yield contributing traits in two mapping
399 populations of bread wheat', *Molecular Breeding*. Springer Netherlands, 19(2), pp. 163–177.
400 doi: 10.1007/s11032-006-9056-8.

401 Li, A. *et al.* (2018) 'Synthetic Hexaploid Wheat: Yesterday, Today, and Tomorrow',
402 *Engineering*. Elsevier, 4(4), pp. 552–558. doi: 10.1016/J.ENG.2018.07.001.

403 Liu, X. *et al*. (2013) 'Mapping QTLs for seedling root traits in a doubled haploid wheat
404 population under different water regimes', *Euphytica*. Springer Netherlands, 189(1), pp. 51–66.
405 doi: 10.1007/s10681-012-0690-4.

406 Lynch, J. *et al*. (1995) 'Root Architecture and Plant Productivity.', *Plant physiology*. American
407 Society of Plant Biologists, 109(1), pp. 7–13. doi: 10.1104/pp.107.1.7.

408 Ma, Z., Bykova, N. V. and Igamberdiev, A. U. (2017) 'Cell signaling mechanisms and metabolic
409 regulation of germination and dormancy in barley seeds', *The Crop Journal*. Elsevier, 5(6), pp.
410 459–477. doi: 10.1016/J.CJ.2017.08.007.

411 Mayer, K. X. (2014) 'A chromosome-based draft sequence of the hexaploid bread wheat
412 (Triticum aestivum) genome.', *Science (New York, N.Y.)*. American Association for the
413 Advancement of Science, 345(6194), p. 1251788. doi: 10.1126/science.1251788.

414 Meister, R. *et al*. (2014) 'Challenges of modifying root traits in crops for agriculture.', *Trends in*
415 *plant science*. Elsevier, 19(12), pp. 779–88. doi: 10.1016/j.tplants.2014.08.005.

416 Mergoum, M. *et al*. (2009) 'Breeding for CLEARFIELD Herbicide Tolerance: Registration of
417 "ND901CL" Spring Wheat', *Journal of Plant Registrations*. Crop Science Society of America,
418 3(2), pp. 170–174. doi: 10.3198/jpr2008.08.0489crc.

419 Pound, M. P. *et al*. (2013) 'RootNav: navigating images of complex root architectures.', *Plant*
420 *physiology*. American Society of Plant Biologists, 162(4), pp. 1802–14. doi:
421 10.1104/pp.113.221531.

422 Richard, C. *et al*. (2015) 'High-throughput phenotyping of seminal root traits in wheat', *Plant*
423 *Methods*. BioMed Central, 11(1), p. 13. doi: 10.1186/s13007-015-0055-9.

424 Shewry, P. R. (2009) 'Wheat', *Journal of Experimental Botany*. Oxford University Press, 60(6),
425 pp. 1537–1553. doi: 10.1093/jxb/erp058.

426 Shu, K. *et al*. (2016) 'Two Faces of One Seed: Hormonal Regulation of Dormancy and
427 Germination', *Mol. Plant*, 9, pp. 34–45. doi: 10.1016/j.molp.2015.08.010.

428 Smith, S. and De Smet, I. (2012) 'Root system architecture: insights from Arabidopsis and cereal
429 crops', *Philosophical Transactions of the Royal Society B: Biological Sciences*, 367(1595), pp.
430 1441–1452. doi: 10.1098/rstb.2011.0234.

431 Weiss, E. and Zohary, D. (2011) 'The Neolithic Southwest Asian Founder Crops', *Current*
432 *Anthropology*. The University of Chicago PressWenner-Gren Foundation for Anthropological
433 Research, 52(S4), pp. S237–S254. doi: 10.1086/658367.

434 Xie, Q. *et al*. (2017) 'Identifying seedling root architectural traits associated with yield and yield
435 components in wheat', *Annals of Botany*, 119(7), pp. 1115–1129. doi: 10.1093/aob/mcx001.

436 Yu, M. *et al*. (2015) 'Quantitative trait locus mapping for growth duration and its timing
437 components in wheat', *Molecular Breeding*. Springer Netherlands, 35(1), p. 44. doi:
438 10.1007/s11032-015-0201-0.

439 YU, M. *et al*. (2014) 'QTLs for Waterlogging Tolerance at Germination and Seedling Stages in
440 Population of Recombinant Inbred Lines Derived from a Cross Between Synthetic and

441 Cultivated Wheat Genotypes', *Journal of Integrative Agriculture*. Elsevier, 13(1), pp. 31–39.
442 doi: 10.1016/S2095-3119(13)60354-8.

443 ZADOKS, J. C., CHANG, T. T. and KONZAK, C. F. (1974) 'A decimal code for the growth
444 stages of cereals', *Weed Research*. Wiley/Blackwell (10.1111), 14(6), pp. 415–421. doi:
445 10.1111/j.1365-3180.1974.tb01084.x.

446

447

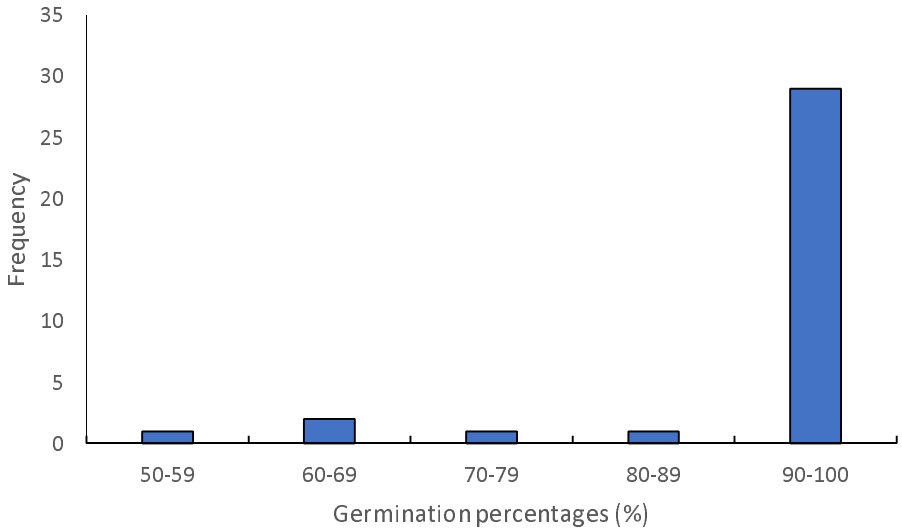

448

449 Supplementary Figure 1. Frequency distribution of the germination potentials (percentage) of the
450 wheat accessions evaluated

451

452 Supplementary Figure 2. The frequency histograms of measured root traits

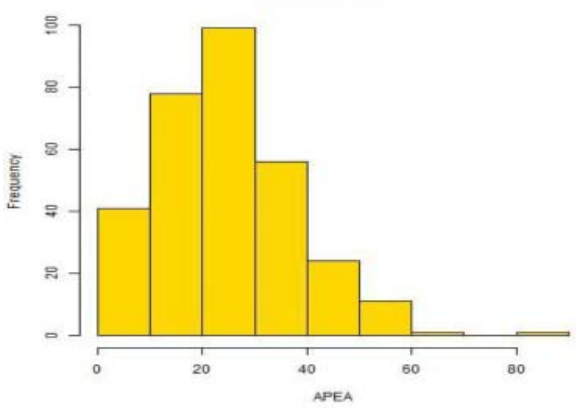

Average primary emergence angle

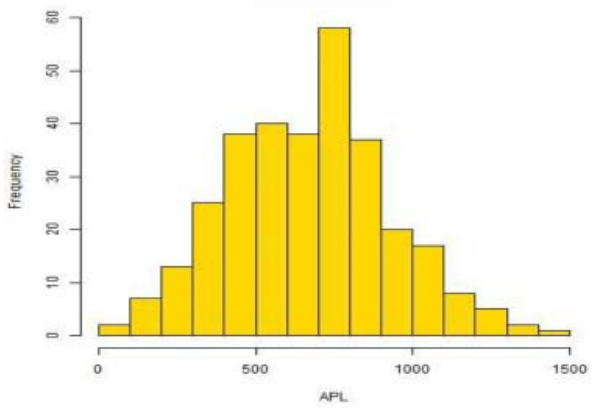

Average primary length

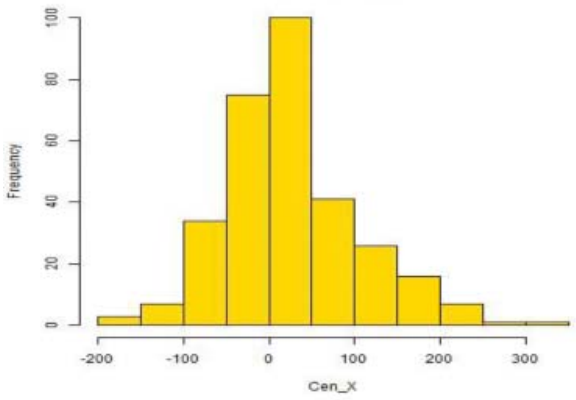

Horizontal co-ordinates of centroid

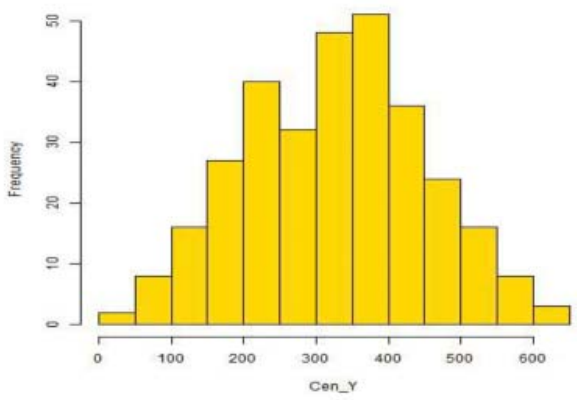

Vertical co-ordinates of centroid

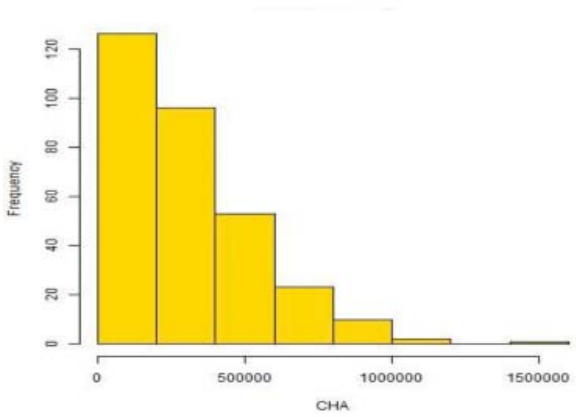

Convex hull area

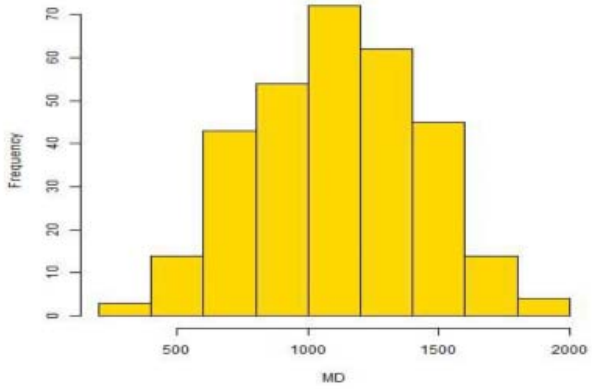

Maximum depth

453

454

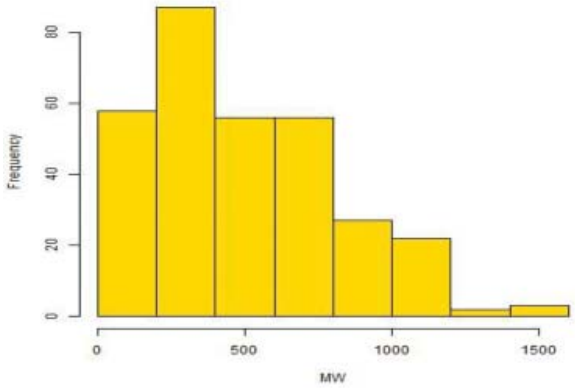

Maximum width

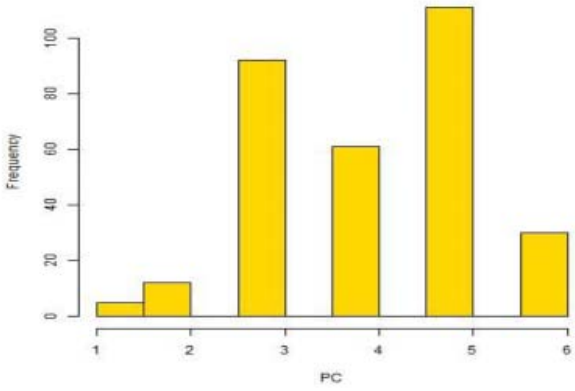

Primary count

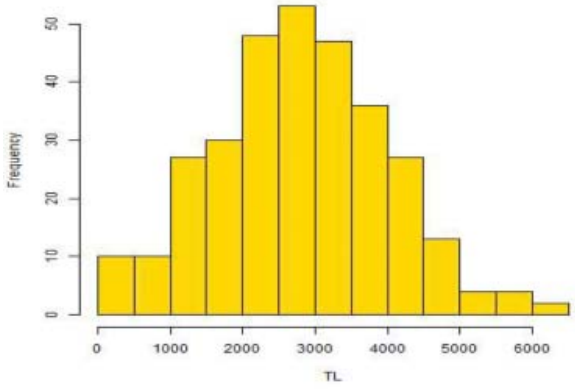

Total length

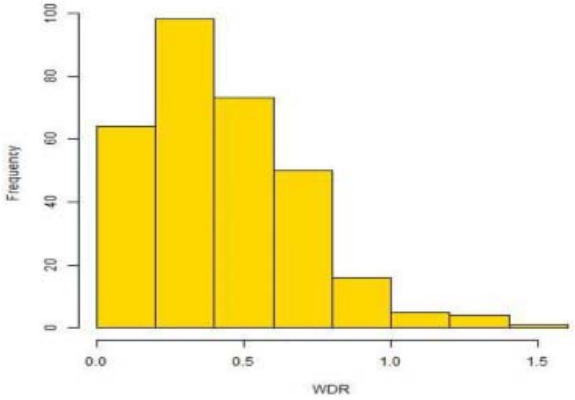

Width-depth ratio

455

456 Supplementary Figure 3. Correlation matrix of the measured root traits.

457

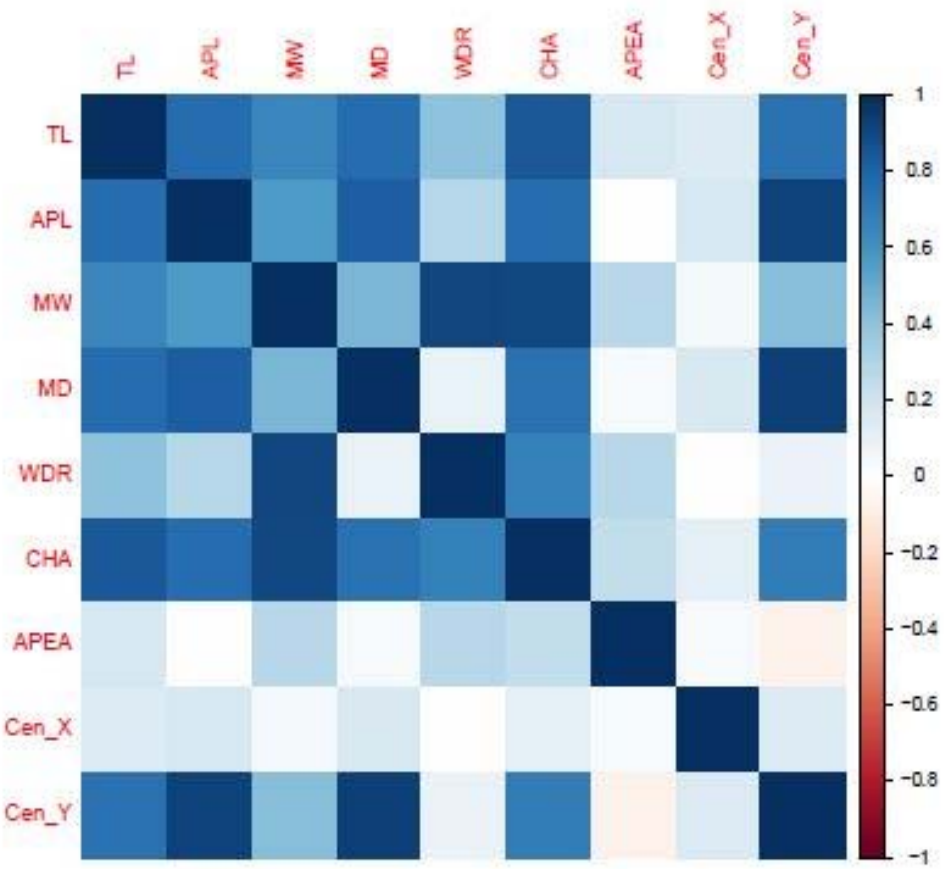

458

459 Abbreviations:

460 TL: Total length

461 APL: Average seminal length

462 MW: Maximum width

463 MD: Maximum depth

464 WDR: Width-depth ratio

465 CHA: Convex hull area

466 APEA: Average seminal emergence area

467 Cen_X: Horizontal coordinates of centroid

468 Cen_Y: Vertical coordinates of centroid

469 PC: Seminal count